



Novel Schiff Base of *E*-2-(((4-Aminophenyl)imino)methyl)-5-(difluoromethoxy)phenol Fluorescence Chemosensor for Detection of Al³⁺, Fe²⁺, Cu²⁺ Ions and its Application towards Live Cell Imaging

MATHIVANAN IYAPPAN^{1,✉}, EZHUMALAI DHINESHKUMAR^{1,✉} and CHINNADURAI ANBUSELVAN^{1,2,*}

¹Department of Chemistry, Annamalai University, Annamalainagar-608002, India

²P.G. and Research Department of Chemistry, Government Arts College, Chidambaram-608102, India

*Corresponding author: E-mail: cas_amu@yahoo.co.in

Received: 13 August 2019;

Accepted: 28 September 2019;

Published online: 25 February 2020;

AJC-19785

A Schiff base compound *E*-2-(((4-aminophenyl)imino)methyl)-5-(difluoromethoxy)phenol was synthesized and characterized by FT-IR, ¹H and ¹³C NMR, ESI-mass spectroscopy. The synthesized compound also selectively detects Al³⁺, Fe²⁺ and Cu²⁺ without any interference of other metal ions. Fluorescence titrations carried out to find the selectivity of Al³⁺, Fe²⁺ and Cu²⁺ in turn-on system, with binding modes of 2:1 complex, confirmed by Job's plot. The presence of metal ions Al³⁺, Fe²⁺ and Cu²⁺ with receptor conformed by ESI-MS spectrum, which changed the base value at 298.00 *m/z*. Moreover, among the binding constant of three metals calculated (20 μM), Al³⁺ showed a high value of 5.7 × 10⁴ M⁻¹ compared to Fe²⁺ and Cu²⁺ metal ions. Prominently, the cytotoxicity activities of probe with HeLa cells were also calculated.

Keywords: Schiff base, Fluorescence, Heavy metals ions, Cytotoxicity.

INTRODUCTION

Among different heavy metal ions, aluminium is a necessary element which is highly abundance in nature and used in each sphere of life such as building equipments, water treatment, packaging utensils, food additives, occupational dusts, pharmaceutical products, electrical components of different gadgets, *etc.* Aluminum is a recognized neurotoxin to organisms [1], causing osteomalacia [2], Alzheimer's disease [3-5] and breast cancer. Consequently, it is essential to adopt highly accurate analytical methods for the detection and control the concentration levels of Al³⁺ in the environmental and biological systems. Available techniques have limitations due to their poor selectivity and sensitivity. Fluorescent sensors are very pretty apparatus for the sensing and recognition of metal ions present in biological environment. These sensors show simplicity, high sensitivity, excellent selectivity and response time [6-10]. The WHO recommended regular human intake of aluminum is around 3-10 mg only [11-13] beyond this limit causes above mentioned diseases.

Iron is an important transition metal ion present in plants and animals. It plays essential role in enzyme catalysis, cellular metabolism, as an oxygen carrier in hemoglobin and as cofactor in few enzymatic reactions [14-16]. However, lesser amount of iron in human body connected to liver and kidney damage, anemia, diabetes, and heart diseases [17]. Hence, various methods to identify the presence of iron in environmental and biological fields get much more attention [18]. In spite of the human body has control over iron amount, recognition and investigation of bioactive iron represents a frightening healthcare challenge. Therefore, researches continuously attempt to increase discovery methods to monitor elemental iron, which include absorption spectra [19,20], magnetic resonance imaging [21], electrochemistry [22,23], HPLC [24] and fluorescence [25-27].

Copper(II) ion plays an essential role in different biological processes. However, high level of copper even for a little period of time may cause gastrointestinal disturbance and long-term consumption able to cause liver or kidney damage [28,29]. In point of weight of the copper ion in biological system, Cu²⁺ ion selective sensors have been progress in recent times [30-

36]. The copper metal ion available in trace amount is essential to human body, it is necessary for few organisms for normal physio-logical processes. For example, enzymes concerned in mitochondria electron transport and melanin production depend on copper ion [37]. In short period, efforts have been dedicated to the progress of high selective and sensitive fluorescent chemo-sensors for sensing and detecting copper ions, and different Cu^{2+} selective fluorescent chemosensors have been reported [38-42]. Most of the model and recently reported Cu^{2+} sensors normally showed low sensitivity [43,44]. In addition, important chemosensors are based on single emission intensity change such as enhancement [45,46] or fluorescence quenching [47,48], it tend to be affected with a different factors such as probe molecule concentration, instrument efficiency and micro-environment [49].

In this work, a Schiff base of (*E*)-2-(((4-aminophenyl)imino)methyl)-5-(difluoromethoxy)phenol (**R**) has been synthesized and successfully applied as fluorescence sensor for Al^{3+} , Fe^{2+} and Cu^{2+} . The cytotoxicity activity of synthesized compound with HeLa cells was also carried out.

EXPERIMENTAL

All the chemicals and solvents were purchased from Sigma-Aldrich (India) and used without further purification. ^1H NMR and ^{13}C NMR spectra recorded on a Bruker-400 MHz spectrometer using TMS as internal standard. Infrared measurements calculated at 4000-400 cm^{-1} region on a Agilent Carry 630 FT-IR spectrometer. Fluorescence measurements conducted on a Hitachi F-4600 fluorescence spectrophotometer with a scan rate of 1200 nm at room temperature.

Synthesis of *E*-2-(((4-aminophenyl)imino)methyl)-5-(difluoromethoxy)phenol (R**):** 1,4-Diaminobenzene (0.30 g, 1.00 mmol) and 4-(difluoromethoxy)-2-hydroxybenzaldehyde (0.45 g, 1.00 mmol) were dissolved in DMSO (20 mL). Then the solution was refluxed for 6 h and cooled at room temperature, a yellow precipitate was filtrated and purified using ethanol to obtain a desired product (**Scheme-I**). Yield: 0.5 g, 60 %. m.p.: 219 °C; IR (KBr, ν_{max} , cm^{-1}): 3440 (O-H), 3338 (N-H), 2965 (Ar-C-H), 2842 (aliph. C-H), 1601 (C=N), 1499 (C=C), 1445 (C-H), 998 (N-H), 863-678 (C-H). ^1H NMR (400 MHz DMSO- d_6): 10.34 (s, OH), 9.97 (s, NH), 8.82 (s, 1H), 7.62-7.63 (t, $J = 1.0$ Hz), 7.41-7.40 (d, $J = 4.0$ Hz), 7.39-7.34 (d, $J = 2.0$ Hz), 7.29 (s, 1H), 7.19 (s, 1H), 6.97 (s, 1H), 5.49 (s, 1H). ^{13}C (100 MHz, DMSO, δ ppm): 158.23, 157.16, 152.99, 140.90, 138.53,

129.78, 124.75, 123.44, 122.10, 120.77, 117.98, 115.52, 112.38, 112.07, 79.12. ESI-MS m/z : Anal. calcd. (found) for $\text{C}_{15}\text{H}_{16}\text{N}_4$ [$\text{M}+\text{H}$] $^+$: 377.42, (376).

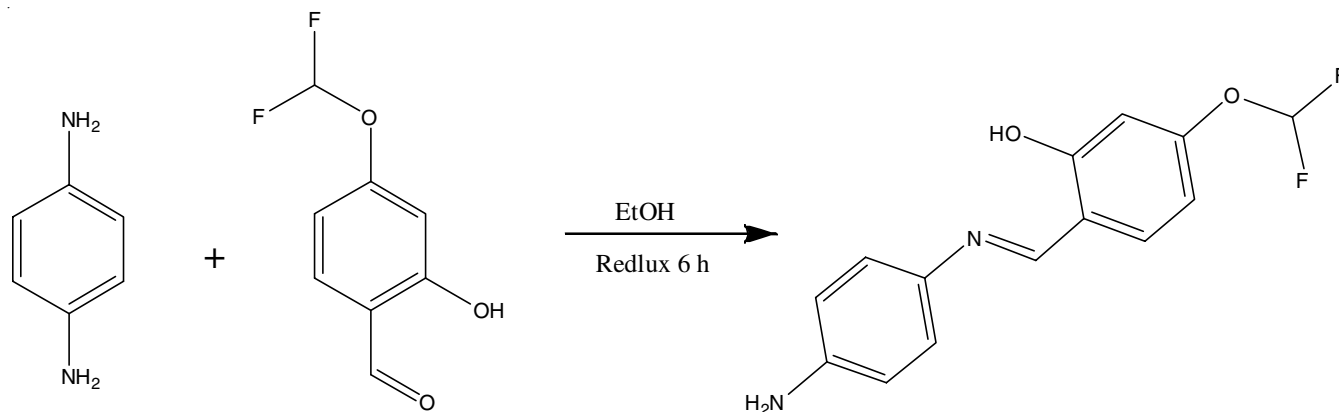
Fluorescence titrations: A stock solution of synthesized compound (probe **R**) (0.005 mmol, 2.05 mg) was prepared in dimethyl sulfoxide (1 mL). A sensor solution (12 μL , 5 mM) was diluted with 2.98 mL methanol to obtain 20 μM . Then, 6-66 μL (20 mM) of $\text{Al}(\text{NO}_3)_3$ (0.02 mmol) dissolved in ethanol (1 mL) solution were transferred to probe **R** (20 μM , 3 mL). After stirring for 5 s, fluorescence spectra were measured. The similar experimental methods were also applied for Fe^{2+} and Cu^{2+} solutions.

UV-visible analysis: Synthesized compound was dissolved in 10 mL ethanol. Various metal ions solutions such as Cu^{2+} , Fe^{3+} , Co^{2+} , Ni^{2+} , Ca^{2+} , Sn^{2+} , Sr^{2+} , Ti^{3+} , V^{3+} , Ti^{3+} , Mn^{2+} , Pb^{2+} , Zn^{2+} , Cd^{2+} , Hg^{2+} , Al^{3+} , Ag^+ and Cr^{3+} (1×10^{-5} M) were prepared and added 50 mL of water solution. Finally, added 0.1 mL these metal ions solution to a test tube containing 0.1 mL of probe **R**, 1:4 ratio of EtOH:H₂O and pH was maintained at 7.0. After few min, spectra were recorded in room at temperature.

Fluorescence spectra: Synthesized compound (probe **R**, 1×10^{-5} M) mixed in ethanol and few min later, 0.1 mL added to each test tube. The fluorescence measurements with various metal ions such as Cu^{2+} , Fe^{3+} , Co^{2+} , Ni^{2+} , Ca^{2+} , Sn^{2+} , Sr^{2+} , Ti^{3+} , V^{3+} , Ti^{3+} , Mn^{2+} , Pb^{2+} , Zn^{2+} , Cd^{2+} , Hg^{2+} , Al^{3+} , Ag^+ and Cr^{3+} (1×10^{-3} M) were performed with the 1:4 ratio of EtOH:H₂O at pH 7.0.

Job's Plot: A stock solution of **R** (0.005 mmol, 1.65 mg) was prepared in ethanol (10 mL). A 100 μL (5 mM) of probe **R** was diluted to 50 mL ethanol to get 20 μM . A 1.6-0.1 mL in a regular interval of the diluted probe **R** were pipetted out and added to quartz cells. A 40 μL (10 mM) of $\text{Al}(\text{NO}_3)_3$ solution was diluted to 50 mL in ethanol then, 0.1-1.6 mL of a diluted Al^{3+} solution was added to each probe **R**. Each cell was filled with ethanol to afford a total volume of 2 mL. After stirring for 10 s, fluorescence spectra were measured. The similar experimental methods were also applied for Fe^{2+} and Cu^{2+} solutions.

Cell culture and cytotoxicity assays: HeLa cells were grown in Dulbecco's modified Eagle's medium (DMEM) supplemented with 10 % FBS. All cells were supplemented with an antibiotic antimycotic solution (100 units mL penicillin, 0.1 mg mL⁻¹ streptomycin and 0.25 mg mL⁻¹ amphotericin B) and grown at 37 °C in standard cell culture conditions (5 % CO₂, 95 % humidity). HeLa cells were cultured in culture media (DMEM, high glucose) in an atmosphere of 5 % CO₂ and 95 % air at 37 °C. The cells



Scheme-I: Synthesis of *E*-2-(((4-aminophenyl)imino)methyl)-5-(difluoromethoxy)phenol (**R**) as fluorescence chemosensor

were seeded into 96-well plates at a density of 4×10^3 cells per well in culture media and then 0, 7.8, 15.6, 31.2, 62.5, 125, 250, 500, 1000 μM (final concentration) of the synthesized compound. The cells were incubated at 37 °C in an atmosphere of 5 % CO_2 and 95 % air for 24 h. The absorbance of cells was measured by ELISA.

RESULTS AND DISCUSSION

Compound **R** was synthesized from 1,4-diaminobenzene and 4-(difluoromethoxy)-2-hydroxybenzaldehyde to form E-2-(((4-aminophenyl)imino)methyl)-5-(difluoromethoxy)phenol (**R**) and characterized by FT-IR, ^1H & ^{13}C NMR, ESI-Mass spectroscopy.

Absorption and fluorescence studies of compound R to Al^{3+} : First of all, to start with fluorescence enhancement studies of compound **R** selectivity (20 μM) to various metal ions such as Cu^{2+} , Fe^{3+} , Co^{2+} , Ni^{2+} , Ca^{2+} , Sn^{2+} , Sr^{2+} , Ti^{3+} , V^{3+} , Tl^{3+} , Mn^{2+} , Pb^{2+} , Zn^{2+} , Cd^{2+} , Hg^{2+} and Ag^+ (10 equiv) in $\text{EtOH}:\text{H}_2\text{O}$, (1:4, v/v, $\text{pH}=7.0$) with HEPES buffer solution with excitation at 368 nm shown in Fig. 1. It is evident that a remarkable enhancement of fluorescence can be detected for Al^{3+} by emitting light yellow fluorescence intensity largely at 478 nm. Furthermore, presence of Fe^{2+} and Cu^{2+} ions with less intensity than Al^{3+} ion with some fluorescence enhancements along with green-yellow fluorescence. Fe^{2+} and Cu^{2+} displayed a slightly red-shifted fluorescence compared to Al^{3+} , which might be due to their heavy mass. In difference, other metal ions displayed no major spectral changes. It seems that the fluorescence enhancement was due to formation of conjugated system after binding metal ions. The fluorescence intensity progressively increased at 510 nm, while excitation value at 385 nm as shown in Fig. 2. The photo-physical property of **R** (20 μM) was studied by variations in UV-visible spectrum of **R** upon treatment with Al^{3+} (Fig. 3). Various concentrations of Al^{3+} to probe **R** solution, an absorbance peak of **R** at 292 nm steadily shifted to 373 nm, which accompanied with clear iso-sbestic points between 240 nm and 343 nm.

The complexation method of $\text{R}-\text{Al}^{3+}$ was investigated using the Job's plot [50,51], which showed a 2:1 ratio binding mode

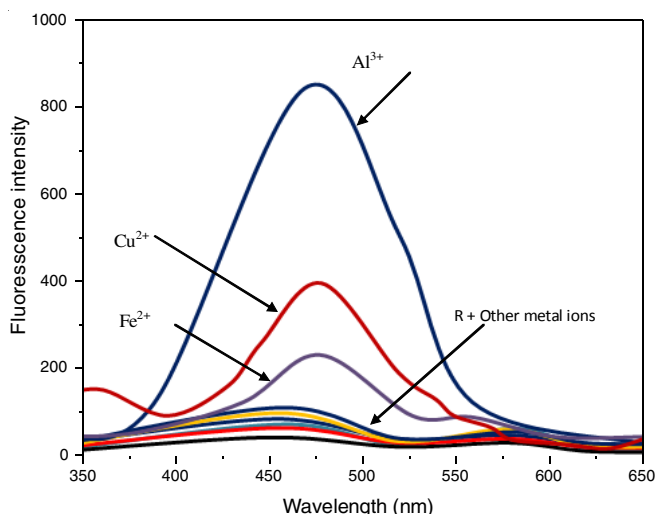


Fig. 1. Fluorescence spectral changes of **R** (20 μM) in the presence of various metal ions (10 equiv.) with an excitation of 328 nm

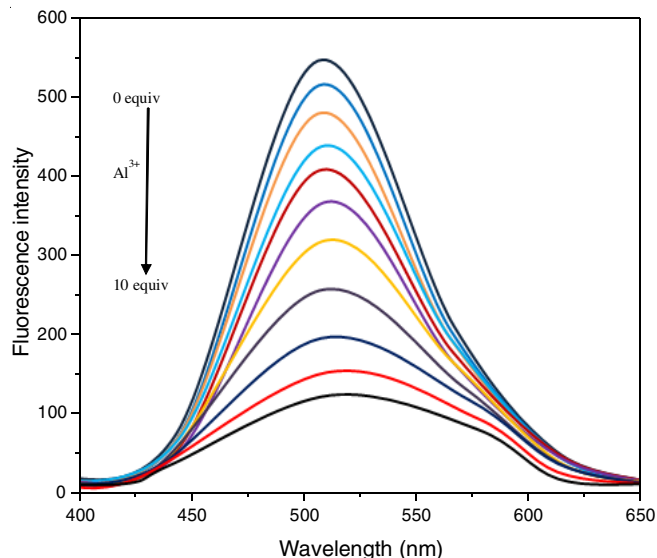


Fig. 2. Fluorescence spectral changes of **R** (20 μM) in the presence of various concentrations of Al^{3+} ions with an excitation of 368 nm

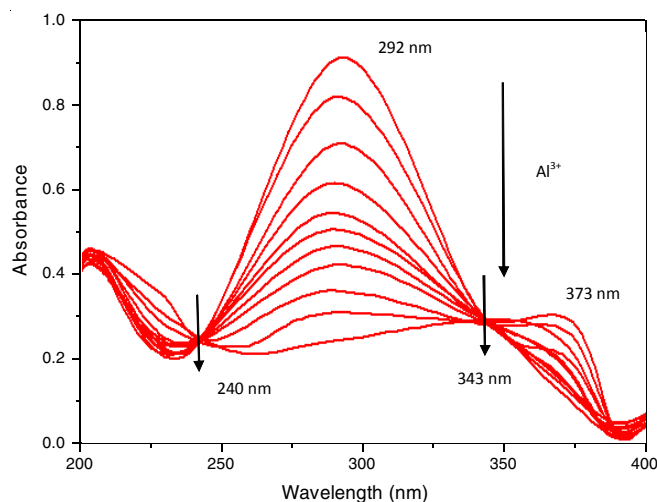


Fig. 3. Absorption spectral changes of **R** (20 μM) in the presence of different concentrations of Al^{3+} ions

of $\text{R}-\text{Al}^{3+}$. The 2:1 complexation between **R** and Al^{3+} was additionally supported by ESI-mass spectrum (Fig. 4), initial peak at $\lambda = 278.25$ nm was indicative of $[2:1+\text{Al}^{3+}-2\text{H}^+]^+$ (calcd. 278.17). From fluorescence titration, a binding constant of **R** with Al^{3+} was calculated and determined as $5.7 \times 10^4 \text{ M}^{-1}$ [52]. The detection limit of **R** for Al^{3+} was found to be 13.38 μM using $3\sigma/\text{slope}$ analysis [53]. When probe **R** (50 μM) solution was treated with Al^{3+} in the presence of various metal ions, moreover, low and high capacity of fluorescence affected by interference metal ions with probe **R** (Fig. 5). In difference Mn^{2+} , Ni^{2+} and Pb^{2+} inhibited 25-45 % of emission intensity of $\text{Al}^{3+}-2:1$, therefore, a fluorescence intensity was still visible in the presence of these metal ions, however, Ca^{2+} , Sn^{2+} , Sr^{2+} , Cd^{2+} and Ag^+ quenched 74, 77, 64, 83 and 61 % of the fluorescence intensity.

Fluorescence studies of R toward Fe^{2+} and Cu^{2+} : The excitation wavelength was changed at 439 nm in order to examine further fluorescent variations of **R** to various metal ions such as Cu^{2+} , Fe^{3+} , Ni^{2+} , Ca^{2+} , Sn^{2+} , Sr^{2+} , V^{3+} , Ti^{3+} , Mn^{2+} , Pb^{2+} , Zn^{2+} ,

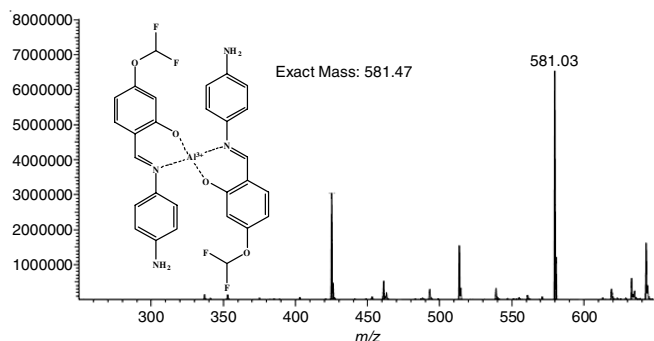


Fig. 4. Positive-ion mass spectrum of **R** (50 μM) upon addition of 1.0 equiv. of $\text{Al}(\text{NO}_3)_3$

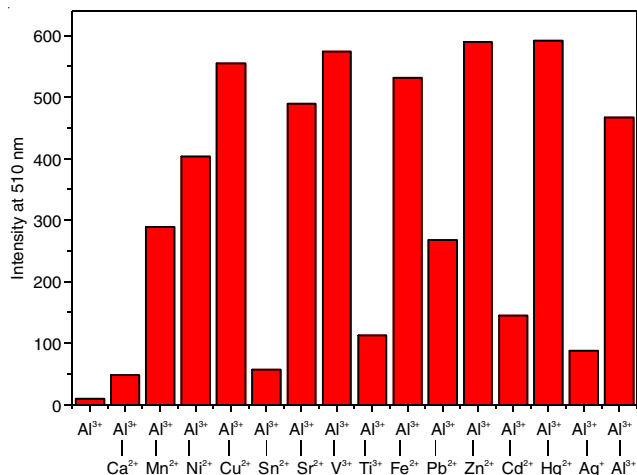


Fig. 5. Competitive metal ions selectivity of **R** (50 μM) commonly added with Al^{3+}

Cd^{2+} , Al^{3+} , Ag^+ and Hg^{2+} (10 equiv.). Enhancement of various metal ions tested, **R** showed remarkable selectivity only for Fe^{2+} and Cu^{2+} by strong fluorescence enhancement at 521 nm (Fig. 6). Furthermore any fluorescence response to other metal ions was not observed. The fluorescence enhancement showed **R** with "turn-on" process to Fe^{2+} and Cu^{2+} in presence of other metal ions. Opportunely, it is possible to discriminate Fe^{2+} and Cu^{2+} through colour change. Most sensors for Al^{3+} , Fe^{2+} and Cu^{2+} generally showed nearly identical fluorescence change at the same position and the same colour change.

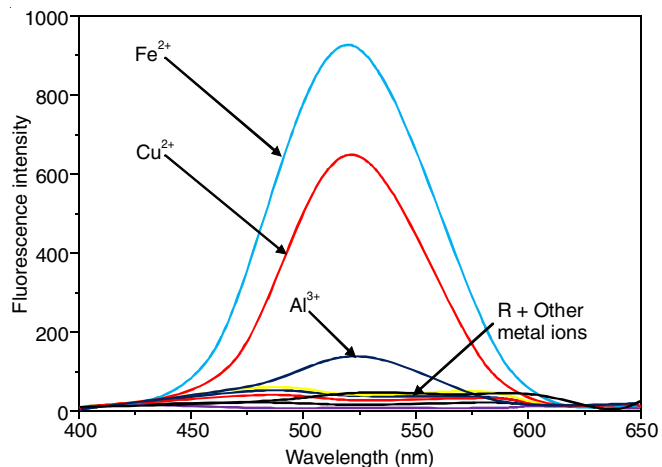


Fig. 6. Fluorescence spectral changes of **R** (20 μM) in the presence of different metal ions

The fluorescence emission intensity at 497 nm constantly increased up to 15 equiv. of Fe^{2+} while excitation wavelength at 438 nm (Fig. 7). Upon gradual addition of Fe^{2+} to the probe **R**, UV-visible titration showed a maximum absorbance decreased at 214 nm, while a new band at 271 nm appeared and saturated with 15 equiv. of Fe^{2+} . In addition, an isosbestic point wavelength at 233 nm indicated the generation of a new stable complex between **R** and Fe^{2+} formed (Fig. 8). To establish a binding stoichiometry of **R**- Fe^{2+} complex, a Job's plot analysis was carried out [50,51], which indicated a 2:1 complex formation between **R**- Fe^{2+} , a maximum absorbance obtained for mole fraction 0.5 μM for a stable complex ($\text{Fe}^{2+}/(\text{R}+\text{Fe}^{2+})$). To confirm the coordination of binding mode of **R** to Fe^{2+} ESI-mass analysis of probe **R** in the presence of Fe^{2+} was also performed. As shown in Fig. 9, a peak at m/z 610.10 could be assigned to $[\text{2:1} + \text{Fe}^{2+} - 2\text{H}^+]^+$ (calcd. 610.09). The association constant (K) of Fe^{2+} -2:1 complex was found to be $5.0 \times 10^4 \text{ M}^{-2}$ using the fluorescence titration data. The recognition of Fe^{2+} not interference other metal ions, so still not enhancement any change, and next low intensity may be attributed Ca^{2+} , V^{2+} and Hg^{2+} due to stability of a stable complex of **R** with Fe^{2+} , more than

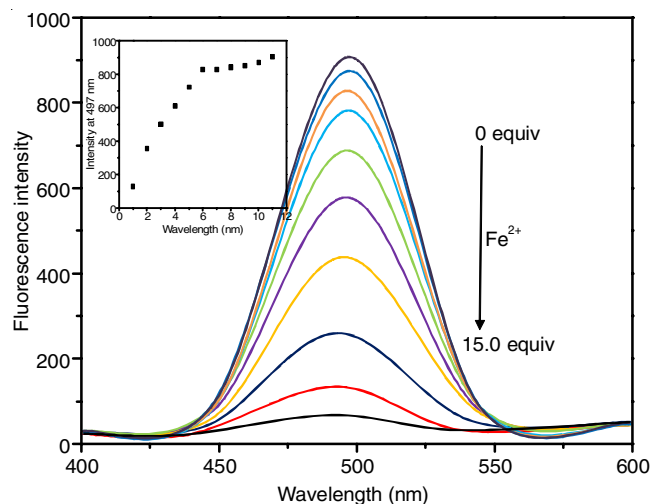


Fig. 7. Emission spectrum of **R** (20 μM) in the presence of different concentrations of Fe^{2+} ion

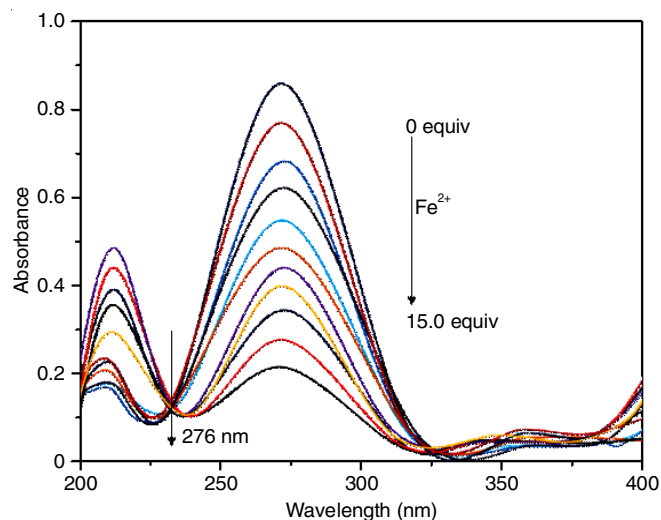


Fig. 8. Absorption spectrum changes of **R** (20 μM) in the presence of different concentrations of Fe^{2+} ion

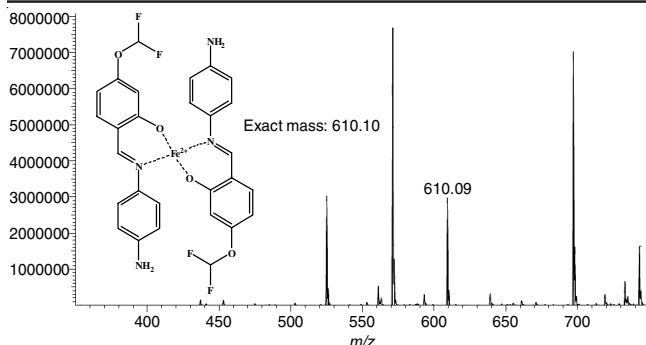


Fig. 9. Positive-ion mass spectrum of **R** (50 μM) upon addition of 1.0 equiv. of $\text{Fe}(\text{NO}_3)_2$

particular metal ion longer wavelength and also not changed binding of Fe^{2+} with probe **R** for Ti^{2+} , Zn^{2+} and Ag^+ ions (Fig. 10).

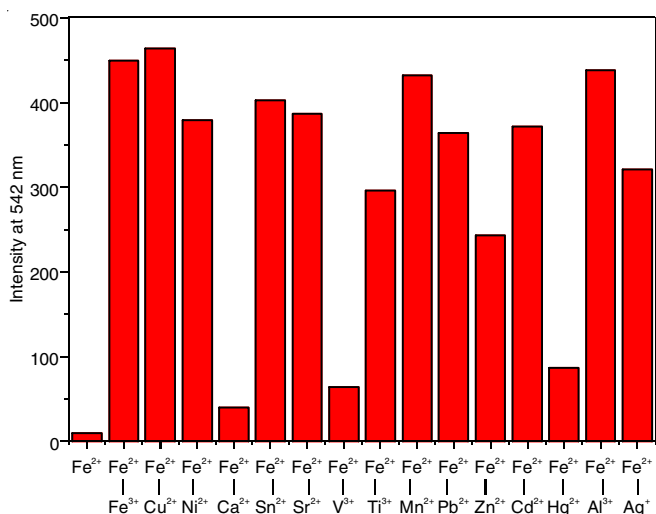


Fig. 10. Competitive selectivity of **R** (20 μM) toward Fe^{2+} in the presence of other metal ions

A fluorescence titration experiment was performed to examine the detecting ability of probe **R** toward Cu^{2+} ions. When probe **R** was titrated with Cu^{2+} ions, a fluorescence emission intensity at 545 nm steadily increased and was saturated at 15 equiv. of Cu^{2+} ions, with excitation value at 473 nm (Fig. 11). To further investigate the interactions between **R** and Cu^{2+} , a UV-vis absorption titration was also examined (Fig. 12). Upon titration with increasing concentration of Cu^{2+} (15 equiv.) to probe **R** solution, absorbance at 340 nm decreased, while a novel red-shifted absorption band at 367 nm gradually appeared. Beyond 15 equiv. Cu^{2+} , the absorbance was saturated with one isosbestic point at 276 nm, indicating a definite binding of **R** with Cu^{2+} ions. An absorbance gradually increases by the gradual addition of Cu^{2+} ions and saturated with increase of 15 equivalents of Cu^{2+} to a fixed concentration of **R** (20 mM). To determine a binding ratio of probe **R** with Cu^{2+} , a Job's plot was constructed and the maximum absorbance was found to be at mole fraction 0.5 μM of $(\text{Cu}^{2+}/(\text{R}-\text{Cu}^{2+}))$ indicating a 2:1 binding ratio between probe **R** and Cu^{2+} [21]. This result was consistent with the ESI-mass analysis (Fig. 13). The positive-ion mass suggested the formation of $[2:1+\text{Cu}^{2+}-2\text{H}^+]^+$ based on the presence of a peak at $m/z = 605.02$ (calcd. 604.57). The association

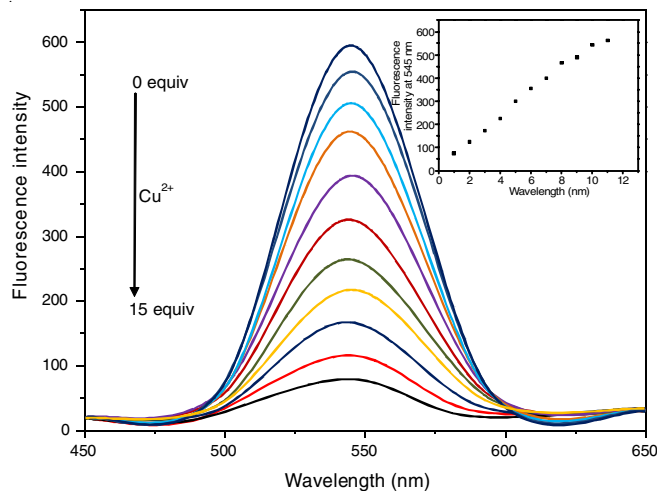


Fig. 11. Emission spectrum of **R** (20 μM) in the presence of different concentrations of Cu^{2+} ions

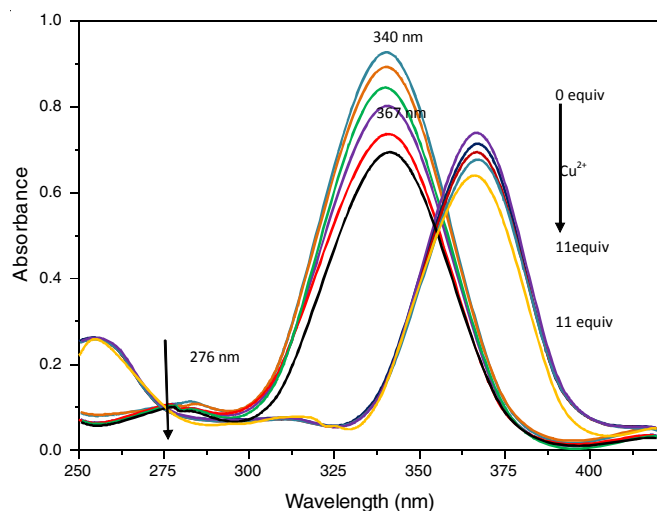


Fig. 12. Absorption spectrum of **R** (20 μM) in the presence of different concentrations of Cu^{2+} ions

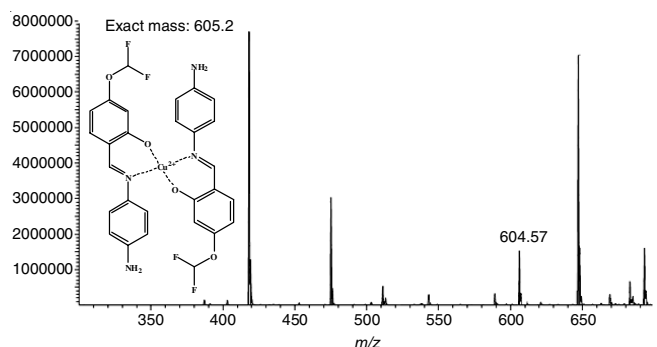


Fig. 13. Positive-ion mass spectrum of **R** (50 μM) upon addition of 1.0 equiv. of $\text{Cu}(\text{NO}_3)_2$

constant was determined to be $5.4 \times 10^4 \text{ M}^{-1}$ for Cu^{2+} ions [39]. However, Ca^{2+} , V^{3+} and Pb^{2+} ions to some extent may interfere, which can probably be due to the fluorescence quenching of these metal ions.

Cytotoxicity with HeLa cells analysis: The cytotoxicity analysis with probe **R** was carried out with HeLa (liver cancer) cell line. HeLa cell treatment with ligand at various concentrations and cell viability were evaluated. HeLa cells were applied

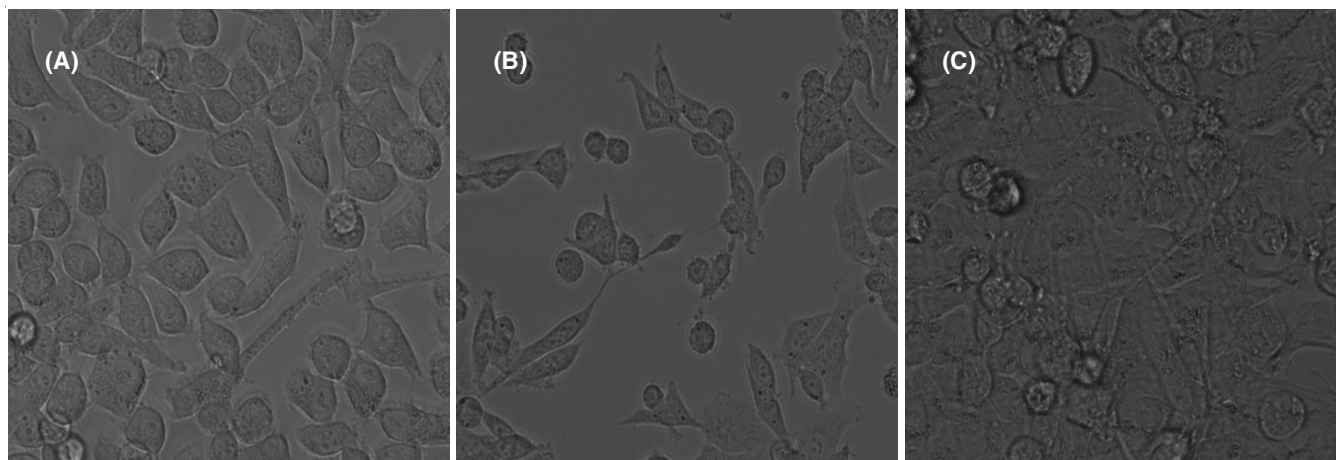


Fig. 14. Cytotoxicity of **R**: (A) before and; (B and C) after treatment with **R** of Hella cell examined by fluorescence microscopy

on the compound and changed their original stability. The cytotoxicity analysis of HeLa cell line with various concentrations such as 0, 7.8, 15.6, 31.2, 62.5, 125, 250, 500 and 1000 μM (final concentration) of ligand was carried out. Moreover, live-cell images before and after treatment incubated at 37 °C in an atmosphere of 5 % CO_2 and 95 % air for 24 h are displayed in Fig. 14. HeLa cells cell viability (%) increased orderly with good response with the ligands. The total concentration of graphical plot of cell viability (%) with different concentration and displayed in Fig. 15. Property of ligands binding with IC_{50} value with short time intervals show good relationship.

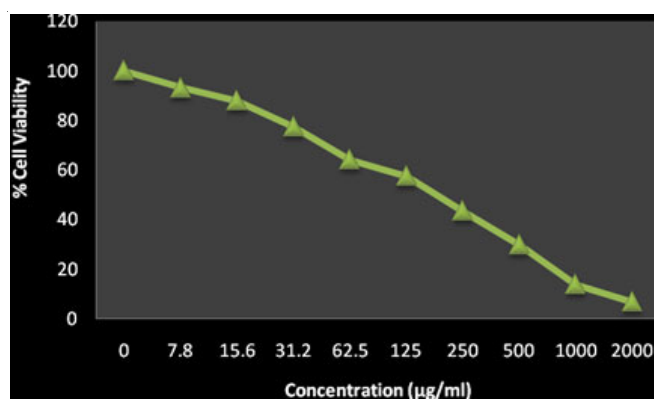


Fig. 15. IC_{50} values of **R** against Hella cell lines

Conclusion

A novel Schiff base multifunctional fluorescent probe **R**, which exhibited high selectivity for trivalent and bivalent ions (Al^{3+} , Fe^{2+} and Cu^{2+}). The sensor could sense and distinguish Al^{3+} , Fe^{2+} and Cu^{2+} through turn-on fluorescence at different wavelengths. The 2:1 binding modes of probe **R** with Al^{3+} , Fe^{2+} and Cu^{2+} were confirmed by Job plots and ESI-mass. The association constants of Fe^{2+} -**R** and Cu^{2+} -**R** complex were maximum reported for the chemosensors to date prominently, as a first report that a chemosensor can selectively discover and differentiate Al^{3+} , Fe^{2+} and Cu^{2+} while several chemosensors reported to date have difficulty in distinguishing Al^{3+} because of their related behaviour. HeLa cell treatment with ligand at various concentrations and cell viability were also evaluated. It was found that HeLa cells cell viability (%) increased orderly

with good response with the ligands and the ligands binding with IC_{50} value with short time intervals showed a good relationship.

CONFLICT OF INTEREST

The authors declare that there is no conflict of interests regarding the publication of this article.

REFERENCES

- M.G. Soni, S.M. White, W.G. Flamm and G.A. Burdock, *Regul. Toxicol. Pharmacol.*, **33**, 66 (2001); <https://doi.org/10.1006/rtp.2000.1441>
- G.C. Woodson, *Bone*, **22**, 695 (1998); [https://doi.org/10.1016/S8756-3282\(98\)00060-X](https://doi.org/10.1016/S8756-3282(98)00060-X)
- D.R. Crapper, S.S. Krishnan and A.J. Dalton, *Science*, **180**, 511 (1973); <https://doi.org/10.1126/science.180.4085.511>
- D.P. Perl and A.R. Brody, *Science*, **208**, 297 (1980); <https://doi.org/10.1126/science.7367858>
- E. House, J. Collingwood, A. Khan, O. Korchazkina, G. Berthon and C. Exley, *J. Alzheimers Dis.*, **6**, 291 (2004); <https://doi.org/10.3233/JAD-2004-6310>
- D.Y. Liu, J. Qi, X.Y. Liu, Z.G. Cui, H.X. Chang, J.T. Chen, H.R. He and G.M. Yang, *Anal. Methods*, **6**, 3578 (2014); <https://doi.org/10.1039/c4ay00641k>
- M. Zhao, L. Ma, M. Zhang, W. Cao, L. Yang and J. Ma, *Spectrochim. Acta A Mol. Biomol. Spectrosc.*, **116**, 460 (2013); <https://doi.org/10.1016/j.saa.2013.07.069>
- L.Y. Yang, Q. Song, K. Damit-Og and H.S. Cao, *Sens. Actuators B Chem.*, **176**, 181 (2013); <https://doi.org/10.1016/j.snb.2012.10.010>
- Z.P. Dong, Y.P. Guo, X. Tian and J.T. Ma, *J. Lumin.*, **134**, 635 (2013); <https://doi.org/10.1016/j.jlumin.2012.07.016>
- S.B. Maity and P.K. Bharadwaj, *J. Lumin.*, **155**, 21 (2014); <https://doi.org/10.1016/j.jlumin.2014.06.020>
- J. Ren and H. Tian, *Sensors*, **7**, 3166 (2007); <https://doi.org/10.3390/s7123166>
- J. Barcelo and C. Poschenrieder, *Environ. Exp. Bot.*, **48**, 75 (2002); [https://doi.org/10.1016/S0098-8472\(02\)00013-8](https://doi.org/10.1016/S0098-8472(02)00013-8)
- Z. Krejpcio and R.W. Wójciak, *Pol. J. Environ. Stud.*, **11**, 251 (2002).
- J.S. Perlmutter, L.W. Tempel, K.J. Black, D. Parkinson and R.D. Todd, *Neurology*, **49**, 1432 (1997); <https://doi.org/10.1212/WNL.49.5.1432>
- K. Soroka, R.S. Vithanage, D.A. Phillips, B. Walker and P.K. Dasgupta, *Anal. Chem.*, **59**, 629 (1987); <https://doi.org/10.1021/ac00131a019>
- P. Aisen, M. Wessling-Resnick and E.A. Leibold, *Curr. Opin. Chem. Biol.*, **3**, 200 (1999); [https://doi.org/10.1016/S1367-5931\(99\)80033-7](https://doi.org/10.1016/S1367-5931(99)80033-7)

17. E. Beutler, V. Felitti, T. Gelbart and N. Ho, *Drug Metab. Dispos.*, **29**, 495 (2001).
18. D. Touati, *Arch. Biochem. Biophys.*, **373**, 1 (2000); <https://doi.org/10.1006/abbi.1999.1518>
19. K.J. Wallace, M. Gray, Z. Zhong, V.M. Lynch and E.V. Anslyn, *Dalton Trans.*, **14**, 2436 (2005); <https://doi.org/10.1039/b504496k>
20. C. Bhaumik, S. Das, D. Maity and S. Baitalik, *Dalton Trans.*, **40**, 11795 (2011); <https://doi.org/10.1039/c1dt10965k>
21. G.M. Brittenham and D.G. Badman, *Blood*, **101**, 15 (2003); <https://doi.org/10.1182/blood-2002-06-1723>
22. T. Isoda, I. Urushibara, H. Sato and N. Yamauchi, *Sensors*, **12**, 8405 (2012); <https://doi.org/10.3390/s120608405>
23. S.E. Andria, C.J. Seliskar and W.R. Heineman, *Anal. Chem.*, **82**, 1720 (2010); <https://doi.org/10.1021/ac902243u>
24. H. Matsumiya, N. Iki and S. Miyano, *Talanta*, **62**, 337 (2004); <https://doi.org/10.1016/j.talanta.2003.08.001>
25. B.P. Espósito, S. Epsztejn, W. Breuer and Z.I. Cabantchik, *Anal. Biochem.*, **304**, 1 (2002); <https://doi.org/10.1006/abio.2002.5611>
26. J.L. Bricks, A. Kovalchuk, C. Trieflinger, M. Nofz, M. Büschel, J. Daub, A.I. Tolmachev and K. Rurack, *J. Am. Chem. Soc.*, **127**, 13522 (2005); <https://doi.org/10.1021/ja050652t>
27. L.J. Fan and W.E. Jones, *J. Am. Chem. Soc.*, **128**, 6784 (2006); <https://doi.org/10.1021/ja0612697>
28. E.L. Que, D.W. Domaille and C.J. Chang, *Chem. Rev.*, **108**, 1517 (2008); <https://doi.org/10.1021/cr078203u>
29. C. Duncan and A.R. White, *Metallomics*, **4**, 127 (2012); <https://doi.org/10.1039/C2MT00174H>
30. L. Quan, T. Sun, T.T. Lin, W.H. Guan, X.G. Zheng, M. Xie and Z.G. Jing, *J. Fluoresc.*, **24**, 841 (2014); <https://doi.org/10.1007/s10895-014-1360-9>
31. S. Chemate and N. Sekar, *RSC Adv.*, **5**, 27282 (2015); <https://doi.org/10.1039/C5RA00123D>
32. P.G. Sutariya, A. Pandya, A. Lodha and S.K. Menon, *Analyst*, **138**, 2531 (2013); <https://doi.org/10.1039/c3an00209h>
33. P. Jiang and Z. Guo, *Coord. Chem. Rev.*, **248**, 205 (2004); <https://doi.org/10.1016/j.cct.2003.10.013>
34. J.S. Kim and D.T. Quang, *Chem. Rev.*, **107**, 3780 (2007); <https://doi.org/10.1021/cr068046j>
35. Z. Xu, J. Yoon and D.R. Spring, *Chem. Soc. Rev.*, **39**, 1996 (2010); <https://doi.org/10.1039/b916287a>
36. P. Kaur and K. Singh, *RSC Adv.*, **4**, 11980 (2014); <https://doi.org/10.1039/C3RA46967K>
37. N. Singh, N. Kaur, B. McCaughan and J.F. Callan, *Tetrahedron Lett.*, **51**, 3385 (2010); <https://doi.org/10.1016/j.tetlet.2010.04.099>
38. G.J. He, X.W. Zhao, X.L. Zhang, H.J. Fan, S. Wu, H.Q. Li, C. He and C.Y. Duan, *New J. Chem.*, **34**, 1055 (2010); <https://doi.org/10.1039/c0nj00132e>
39. S. Khatua, S.H. Choi, J. Lee, J.O. Huh, Y. Do and D.G. Churchill, *Inorg. Chem.*, **48**, 1799 (2009); <https://doi.org/10.1021/ic802314u>
40. C.W. Yu, Y.Y. Wen and J. Zhang, *Sensors*, **14**, 21375 (2014); <https://doi.org/10.3390/s141121375>
41. Y. Jeong and J. Yoon, *Inorg. Chim. Acta*, **381**, 2 (2012); <https://doi.org/10.1016/j.ica.2011.09.011>
42. M.A. Qazi, I. Qureshi and S. Memon, *J. Mol. Struct.*, **975**, 69 (2010); <https://doi.org/10.1016/j.molstruc.2010.03.088>
43. X.L. Ni, X. Zeng, C. Redshaw and T. Yamato, *Tetrahedron*, **67**, 3248 (2011); <https://doi.org/10.1016/j.tet.2011.03.008>
44. S. Patra, R. Lo, A. Chakraborty, R. Gunupuru, D. Maity, B. Ganguly and P. Paul, *Polyhedron*, **50**, 592 (2013); <https://doi.org/10.1016/j.poly.2012.12.002>
45. S. Wu, K. Zhang, Y. Wang, D. Mao, X. Liu, J. Yu and L. Wang, *Tetrahedron Lett.*, **55**, 351 (2014); <https://doi.org/10.1016/j.tetlet.2013.11.024>
46. L.-J. Ma, W. Cao, J. Liu, M. Zhang and L. Yang, *Sens. Actuators B Chem.*, **181**, 782 (2013); <https://doi.org/10.1016/j.snb.2013.01.095>
47. J. Wang, L. Long, D. Xie and X. Song, *Sens. Actuators B Chem.*, **177**, 27 (2013); <https://doi.org/10.1016/j.snb.2012.10.077>
48. B. Tang, T. Yue, J. Wu, Y. Dong, Y. Ding and H. Wang, *Talanta*, **64**, 955 (2004); <https://doi.org/10.1016/j.talanta.2004.04.016>
49. Y.S. Wu, C.Y. Li, Y.F. Li, J.L. Tang and D. Liu, *Sens. Actuators B Chem.*, **203**, 712 (2014); <https://doi.org/10.1016/j.snb.2014.07.046>
50. E. Dhineshkumar, M. Iyappan and C. Anbuselvan, *J. Mol. Struct.*, **1177**, 545 (2019); <https://doi.org/10.1016/j.molstruc.2018.09.088>
51. D. Ezhumalai, I. Mathivanan and A. Chinnadurai, *Spectrochim. Acta A: Mol. Biomol. Spectrosc.*, **199**, 209 (2018); <https://doi.org/10.1016/j.saa.2018.03.053>
52. R. Yang, K. Li, K. Wang, F. Zhao, N. Li and F. Liu, *Anal. Chem.*, **75**, 612 (2003); <https://doi.org/10.1021/ac020467n>
53. Y.-K. Tsui, S. Devaraj and Y.-P. Yen, *Sens. Actuators B Chem.*, **161**, 510 (2012); <https://doi.org/10.1016/j.snb.2011.10.069>